Dominant Negative Pathogenesis by Mutant Proinsulin in the Akita Diabetic Mouse

Tetsuro Izumi,[1] Hiromi Yokota-Hashimoto,[1] Shengli Zhao,[1] Jie Wang,[1] Philippe A. Halban,[2] and Toshiyuki Takeuchi[1]

Autosomal dominant diabetes in the Akita mouse is caused by mutation of the insulin 2 gene, whose product replaces a cysteine residue that is engaged in the formation of an intramolecular disulfide bond. These heterozygous mice exhibit severe insulin deficiency despite coexpression of normal insulin molecules derived from three other wild-type alleles of the insulin 1 and 2 genes. Although the results of our previous study suggested that the mutant proinsulin 2 is misfolded and blocked in the transport from the endoplasmic reticulum to the Golgi apparatus, its dominant negative nature has not been fully characterized. In the present study, we investigated the possible pathogenic mechanisms induced by the mutant proinsulin 2. There is no evidence that the mutant proinsulin 2 attenuates the overall protein synthesis rate or promotes the formation of aberrant disulfide bonds. The trafficking of constitutively secreted alkaline phosphatase, however, is significantly decreased in the islets of Akita mice, indicating that the function of early secretory pathways is nonspecifically impaired. Morphological analysis has revealed that secretory pathway organelle architecture is progressively devastated in the β-cells of Akita mice. These findings suggest that the organelle dysfunction resulting from the intracellular accumulation of misfolded proinsulin 2 is primarily responsible for the defect of coexisting wild-type insulin secretion in Akita β-cells. *Diabetes* 52:409–416, 2003

Defective folding of membrane-bound and soluble proteins is known to be the basis of many inherited diseases (1). Synthesized cargo proteins are first inserted into the endoplasmic reticulum (ER) and are folded with the assistance of a diverse range of ER chaperones. Genetic alterations in the coding sequence affect the folding of cargo proteins and cause either recessive or dominant diseases. Although the basis for the pathogenesis of diseases with recessive inheritance are understood as a deficiency of functional molecules, the mechanism of dominant inheritance is not fully understood.

The Akita mouse, which harbors the autosomal dominant mutation *Mody*, shows hyperglycemia with notable pancreatic β-cell dysfunction (2). We recently demonstrated that a mutation in the insulin 2 gene (*Ins2*; Cys96Tyr) that results in a disruption of an intramolecular disulfide bond is responsible for the phenotype of the Akita mouse (3). The mutant proinsulin 2 is thought to be improperly folded based on the following observations (3). First, the expression levels of ER-resident chaperones, such as BiP and protein disulfide isomerase, are increased in the β-cells of Akita mice. The transcriptional induction of ER chaperone genes is a well-known response to misfolded proteins and is termed "the unfolded-protein response" (4,5). Second, electron microscopic analysis of the β-cells has revealed that the lumina of ER-like organelles are markedly enlarged and have a more electron-dense appearance, suggesting that misfolded proinsulin 2 is trapped and accumulated. Third, exogenously expressed mutant proinsulin 2 is scarcely secreted from CHO cells in contrast to the wild type, presumably consequent to action of the quality control mechanisms that normally allow only properly folded proteins to exit the ER and progress in the secretory pathway (6). Furthermore, recent physicochemical and structural analyses of insulin analogs lacking the A7–B7 disulfide bond show that the linkage is crucial for maintaining the native conformation and biological activity (7,8). All these findings indicate that C96Y proinsulin 2 is misfolded and evokes so-called conformational diseases (1). The diabetic phenotype of heterozygous Akita mice, however, cannot be simply explained by the selective secretion block and degradation of mutant proinsulin 2, because there are coexisting normal insulin molecules derived from three other wild-type alleles of insulin 1 (*Ins1*) and 2 genes. If these normal insulin molecules are secreted efficiently, severe glucose intolerance and insulin deficiency should not occur in Akita mice. Although there is no gross defect in transcription from the wild-type insulin alleles in the β-cells of Akita mice, the protein levels of proinsulin and insulin are diminished to such a degree that the loss of only mutant insulin could not account for it (3).

It has recently been shown that the number of apoptotic cells in islets of Akita mice is much larger than in control islets and that targeted disruption of the CHOP/Gadd153 gene ameliorates the diabetes of Akita mice (9). The CHOP gene encodes a transcription factor that promotes apopto-

From the [1]Department of Molecular Medicine, Institute for Molecular and Cellular Regulation, Gunma University, Maebashi, Japan; and the [2]Louis-Jeantet Research Laboratories, University Medical Centre, Geneva, Switzerland.

Address correspondence and reprint requests to Dr. Tetsuro Izumi, Department of Molecular Medicine, Institute for Molecular and Cellular Regulation, Gunma University, 3-39-15 Showa-machi, Maebashi, Gunma 371-8512, Japan. E-mail: tizumi@showa.gunma-u.ac.jp.

Received for publication 1 August 2002 and accepted in revised form 5 November 2002.

Current address for J.W. is Department of Biochemistry and Molecular Biology, University of Chicago, Chicago, IL 60637.

ER, endoplasmic reticulum; SEAP, secretory alkaline phosphatase; TUNEL, transferase-mediated dUTP nick-end labeling.

sis in response to ER stress (10,11). Thus these findings indicate that the CHOP-dependent cell death pathway involves the pathogenesis of diabetes in Akita mice. It is notable, however, that a background null mutation in CHOP only delays the onset, but does not prevent the eventual development of diabetes in heterozygous *Ins2*$^{WT/C96Y}$ Akita mice (9). Furthermore, it does not produce any beneficial effects on the diabetic phenotype of homozygous *Ins2*$^{C96Y/C96Y}$ mice, despite the fact that loss of both copies of *Ins2* is fully compensated for by *Ins1* (12). Therefore, CHOP-independent cell death pathways or other unrelated mechanisms causing β-cell dysfunction in Akita mice must exist.

In the present study, we investigated several pathogenic mechanisms that may occur in the β-cells of Akita mice, at the molecular, organellar, and cellular levels. We demonstrated a significant decrease in the transport efficiency of secretory alkaline phosphatase (SEAP), which is completely unrelated to insulin and is secreted in a constitutive manner. Furthermore, we observed a deterioration of organelle architecture that universally and progressively occurs in β-cells. These findings indicate that mutant proinsulin 2 in Akita mice causes generalized organelle dysfunction in the secretory pathways of individual β-cells.

RESEARCH DESIGN AND METHODS

Mice and pancreatic islet preparation. All animal experiments were performed in accordance with the rules and regulations of the Animal Care and Experimentation Committee, Gunma University, Showa Campus. Heterozygous Akita mice (C57BL/6 background) and control C57BL/6 mice were bred and fed as previously described (3). Pancreatic islets were isolated by pancreatic duct injection of collagenase solution, as previously described (3).

DNA constructs and site-directed mutagenesis. Mouse *Ins2* cDNA that harbors both C96Y and C31A mutations was prepared as previously described (13). Two DNA fragments that overlap the mutation site C31A were amplified with the primers (5′-GCCAAGCTTAAGTGATCCGCTACAATCAA-3′ and 5′-GTGCTGCTTGACAAAAGCCT-3′; and 5′-CAAGCAGCACCTTGCTGGTTCCCA CC-3′ and 5′-GCGGGATCCATCGATGCTCATTCAAAGGTTTTATTC-3′) using *Ins2*^{C96Y} cDNA as a template. The resultant products were digested with *Hin*dIII and *Fnu*4HI and with *Fnu*4HI and *Bam*HI, respectively, and were ligated together into the *Hin*dIII and *Bam*HI sites of the pcDNA3 vector.

CHO cell lines expressing wild-type or mutant insulin genes. Transfections were performed using Lipofectamin 2000 reagent (Invitrogen, Groningen, the Netherlands). Except for the clones w9 and a7 as previously described (3), the CHO cell clones labeled "w," "a," and "d," which express wild-type, C96Y single mutant, and C96Y and C31A double mutant mouse insulin 2, respectively, were newly established in the presence of 0.8 mg/ml Geneticin (Sigma Chemical, St. Louis, MO). Proinsulin in cell extracts and the media were analyzed by immunoblotting using guinea pig anti-rat C-peptide antibodies (Linco Research, St. Charles, MO), as previously described (3).

Two-dimensional gel electrophoresis. One- and two-dimensional SDS-PAGE was performed to study nascent chains, as previously described (14), with modifications. Nonreduced immunoprecipitate samples were loaded in the first-dimension gel. After electrophoresis in the first dimension, each gel strip was incubated in sample buffer containing 100 mmol/l dithiothreitol at 95°C for 10 min and placed on top of the second-dimension slab gel.

Secretion assays of insulin and SEAP. Isolated pancreatic islets were cultured overnight in RPMI 1640 medium supplemented with 10% FCS, 100 units/ml penicillin, and 100 μg/ml streptomycin. The islets were infected with the recombinant adenovirus encoding SEAP (15) at 100 multiplicity of infection (assuming that one islet contained 1,000 cells) in 0.5 ml medium for 1 h and then further cultured in a 6-cm dish for 24 h. Then 20 islets were transferred to a microcentrifuge tube and incubated for 30 min in modified Krebs-Ringer buffer (120 mmol/l NaCl, 5 mmol/l KCl, 24 mmol/l $NaHCO_3$, 1 mmol/l $MgCl_2$, 2 mmol/l $CaCl_2$, 15 mmol/l HEPES [pH 7.4], and 0.1% BSA). The islets were then incubated for 30 min in the same buffer, followed by 30 min in the buffer modified to include high K^+ (60 mmol/l KCl, 65 mmol/l NaCl). At the time of each medium change, the islets were sedimented by centrifugation at 800*g* for 5 min, and the media were collected and again centrifuged for 5 min to remove any cell debris. Immunoreactive insulin was measured using guinea pig anti-porcine insulin antibodies, as previously described (3). The SEAP assay was performed according to the method described previously (16). Cell extracts were sonicated for 10 s and centrifuged for 10 min at 10,000 rpm. Samples (media and cell extracts) were heated at 65°C for 5 min to inactivate the endogenous phosphatases, transferred to new tubes, and diluted to 200 μl with SEAP buffer (1 mol/l diethanolamine, 0.5 mmol/l $MgCl_2$, 10 mmol/l L-homoarginine). After preincubation for 10 min at 37°C in a 96-well plate, the SEAP substrate (20 μl of 120 mmol/l *p*-nitrophenyl phosphate; Sigma Chemical) was added to the samples. The light absorbance at 405 nm (A_{405}) was measured using an enzyme-linked immunosorbent assay microplate reader (MTP500; Corona Electric, Hitachi, Japan).

Electron microscopy. Mice were anesthetized and perfused transcardially for 20 min with 2% glutaraldehyde–2% paraformaldehyde in 0.1 mol/l phosphate buffer (pH 7.4), and immersed for 1 day at 4°C in the same buffer. Tissue preparation and electron microscopy were performed as previously described (3).

Transferase-mediated dUTP nick-end labeling assay. Mice were perfused for 15 min with 4% paraformaldehyde in 0.1 mol/l phosphate buffer (pH 7.4). The pancreata were further fixed in the same solution at 4°C overnight and embedded in paraffin. Serial paraffin sections (4 μm thick) were prepared. Apoptotic cells were detected by transferase-mediated dUTP nick-end labeling (TUNEL) assay using the fluorescein-apoptosis detection kit from Promega (Madison, WI). Only after the whole islet was examined in the serial sections were the apoptotic cells counted and included in the assay. Islets <50 μm in diameter were not included.

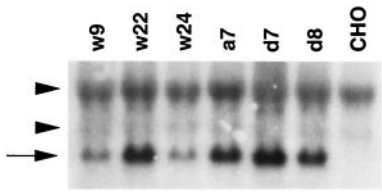

FIG. 1. Northern blot analysis of CHO cell lines expressing wild-type or mutant mouse insulin 2. Total RNA (20 μg) isolated from each clone or from the parental CHO cells were electrophoresed, transferred to a nylon membrane, and hybridized with a mouse insulin 2 cDNA. Arrow indicates the position of insulin transcripts. Arrowheads indicate the position of 28 S and 18 S ribosomal RNA that were nonspecifically hybridized with the probe. Individual CHO cell clones expressed the following forms of insulin: w9, w22, and w24, the wild type; a7, the C96Y (A7) single mutant; and d7 and d8, the C96Y (A7) and C31A (B7) double mutant.

RESULTS

Effect of a proteasome inhibitor on proinsulin turnover in CHO cells. Misfolded secretory proteins undergo retrograde translocation from the ER and are then hydrolyzed by the ER-associated ubiquitin-proteasome system (17). To examine whether the C96Y mutant proinsulin 2 found in Akita mice is indeed misfolded and degraded by the proteasome, CHO cell lines expressing *Ins2*^{WT} or *Ins2*^{C96Y} were pulse-labeled with [^{35}S]methionine, and the effect on intracellular proinsulin turnover of lactacystin, which is a specific and potent inhibitor of the proteasome (18), was investigated. Because nonendocrine CHO cells lack prohormone conversion endopeptidase to process proinsulin to insulin and secretory granules to store insulin, proinsulin that is synthesized and folded in the ER is constitutively secreted, which makes it possible to directly measure the transport efficiency of proinsulin from the ER to the Golgi apparatus. We previously demonstrated that the C96Y mutant proinsulin 2 is secreted at much lower levels than the wild type in these cells (3) (see also Fig. 5). Consistent with the findings of Northern blot analysis (Fig. 1), similar amounts of newly synthesized wild-type and C96Y proinsulin 2 (8.6 kDa) were immunoprecipitated immediately after the pulse in the clones w22 and a7,

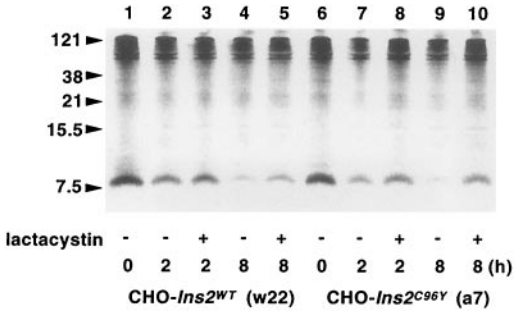

FIG. 2. Effect of a proteasome inhibitor, lactacystin, on the intracellular turnover of newly synthesized proinsulin 2. Metabolic labeling and immunoprecipitation were performed as previously described (3). Briefly, CHO cell lines expressing either wild-type (clone w22) or C96Y mutant insulin 2 (clone a7) were radiolabeled with 100 μCi [^{35}S]methionine. Either immediately after the pulse or after chasing for the indicated times with or without 20 μmol/l lactacystin (Calbiochem-Novabiochem, La Jolla, CA) at 37°C, the cell extracts were immunoprecipitated with anti–C-peptide antibodies. Immune complexes were analyzed by tricine-SDS-PAGE (16.5% polyacrylamide gel).

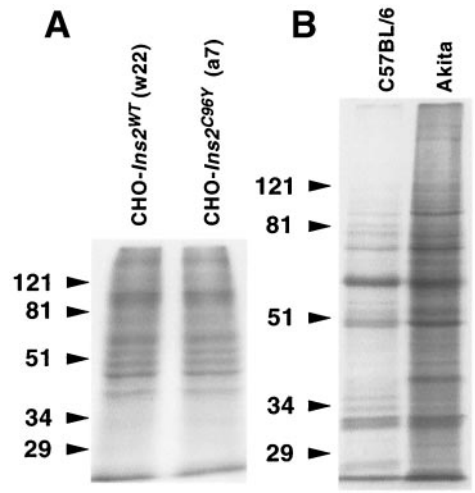

FIG. 3. Protein synthesis levels in CHO cell lines and pancreatic islets. CHO cell lines expressing either wild-type (clone w22) or C96Y mutant insulin 2 (clone a7) (*A*), or pancreatic islets isolated from 16-week-old male control C57BL/6 and Akita mice (*B*) were labeled for 30 min with [^{35}S]methionine. Islets (n = 200) of similar sizes from each mouse strain were used. An equal amount of the cell extract protein (50 μg) was loaded onto 10% polyacrylamide gel and analyzed by fluorography.

respectively (Fig. 2, *lanes 1* and *6*). Lactacystin facilitated the retention of C96Y proinsulin 2 in cells after the chase for 2 and 8 h, although the same treatment had a negligible or weak effect on the wild-type proinsulin 2. We could not estimate the fraction of proinsulin that was actually degraded because quantitative immunoprecipitation was difficult from the media containing FCS, which must be included during the chase to keep the cells active for protein synthesis. Nonetheless, differences in the effect of lactacystin on the intracellular turnover of wild-type and mutant proinsulin 2 suggested that a significant portion of nascent C96Y proinsulin 2 was misfolded and degraded by the proteasome.

Protein synthesis levels in CHO cells and pancreatic islets expressing mutant insulin. The selective degradation of mutant proinsulin 2 by the proteasome, however, does not explain the profound reduction in protein levels of coexisting wild-type proinsulin and insulin in Akita β-cells (3). The presence of misfolded proteins in the ER elicits coordinated controls of gene transcription and translation to relieve the demands made on the organelle (4,5). One of these responses consists of a repression of protein synthesis that involves phosphorylation of the α-subunit of eukaryotic initiation factor-2 by an ER-resident kinase, PEK/PERK (19,20). A profound translational attenuation might decrease the synthesis of insulin itself or of other molecules that are required for the integrity of host cells, thereby affecting insulin secretion in Akita β-cells. Neither proinsulin nor overall protein synthesis rates, however, were decreased in CHO cells expressing *Ins2*^{C96Y} compared with those expressing *Ins2*^{WT} (Fig. 2, *lanes 1* and *6*, and Fig. 3*A*). Furthermore, the overall protein synthesis rate in islets isolated from Akita mice was not decreased (Fig. 3*B*). The amount of radiolabel incorporation into acid-insoluble materials in Akita islets was increased 2.9-fold compared with that in control islets. The apparent increase in protein synthesis may have been caused by the chronic exposure of Akita islets to hyperglycemia in vivo. These findings preclude the possibility of a profound reduction in protein synthesis by mutant proinsulin 2.

Intramolecular and intermolecular disulfide bond formation of proinsulin 2. The presence of disulfide-bonded proinsulin aggregates in Akita islets was previously suggested because a high level of anti–C-peptide immunoreactivity was preferentially recovered at the boundary between stacking and resolving gels under nonreducing conditions, although it was also found at a lower level in control islets (3). We investigated the formation of disulfide bonds involving wild-type and mutant proinsulin using a two-dimensional SDS-PAGE system described elsewhere (14). Labeled material just below the diagonal that migrated to the position corresponding to the molecular weight of monomeric proinsulin 2 was found in both wild-type and C96Y proinsulin 2 immunoprecipitates (Fig. 4*A*, arrowheads with "m"), consistent with the presence of intramolecular disulfide bonds. Just above these spots, several other radiolabeled products that are considered to be proinsulin oligomers or proinsulin cross-linked to other proteins were observed (Fig. 4*A*, arrowheads with asterisks). Although the quenching method with *N*-ethylmaleimide might not fully preclude thiol-disulfide rearrangement during the trapping procedure, the overall patterns of radioactive spots were not significantly different between wild type and mutant proinsulin 2. Moreover, incubation with lactacystin during the chase period to prevent the degradation of misfolded proinsulin molecules did not change the overall patterns (data not shown), suggesting that these intermolecular disulfide bonds can eventually be reduced and corrected before exporting from the ER to the proteasome.

The expression levels of the insulin gene in our CHO cell clones were much lower than those in the pancreatic islets (data not shown). The low concentration in the ER might have prevented the mutant proinsulin from forming aberrant intermolecular disulfide bonds in CHO cells. To exclude this possibility, we next performed the same analysis using isolated pancreatic islets. Radioactive spots containing intermolecular disulfide bonds were clearly observed in the control islets (Fig. 4*B*), suggesting that these bonds are physiologically formed during the normal folding process of proinsulin. Although the radioactivity

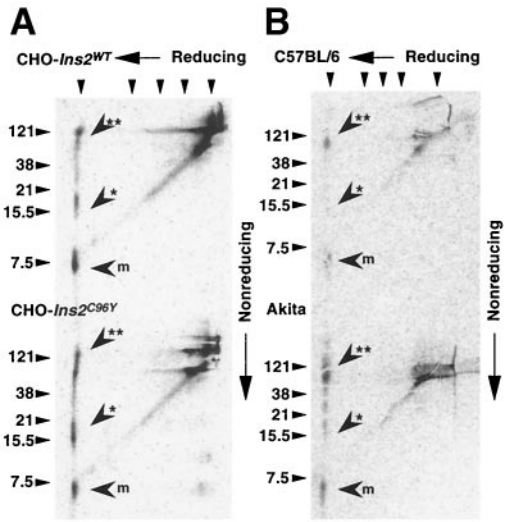

FIG. 4. Assessment of intra- and intermolecular disulfide bonds within proinsulin 2. *A*: CHO cell lines expressing either wild-type (clone w22; *upper panels*) or C96Y mutant mouse insulin 2 (clone a7; *lower panels*) were labeled for 30 min with [^{35}S]methionine. The cells were flooded with PBS containing 20 mmol/l *N*-ethylmaleimide to alkylate free sulfhydryls, and solubilized in the continued presence of *N*-ethylmaleimide to prevent postlysis oxidation of free cysteines and trap disulfides. The nascent proinsulin 2 was isolated by immunoprecipitation with anti–C-peptide antibodies. The immune complexes were then analyzed by two-dimensional tricine-SDS-PAGE (16.5% polyacrylamide gel without urea). Arrowheads with "m" indicate monomeric proinsulin 2 that has only intramolecular disulfide bonds. Judging from the migration of the spots, arrowheads with one asterisk probably correspond to dimeric proinsulin 2 molecules that are connected by intermolecular disulfide bonds. Arrowheads with two asterisks indicate proinsulin 2 molecules that had intermolecular disulfide bonds with other proteins or multiple proinsulin 2 molecules. *B*: Pancreatic islets (n = 250) isolated from 16-week-old male control C57BL/6 and Akita mice were preincubated with methionine-free DMEM for 1 h and then pulse-labeled with [^{35}S]methionine for 1 h. They were further chased for 2 h and analyzed as described above.

associated with these spots appeared higher in Akita islets than in control islets (Fig. 4*B*), the quantitative comparison was difficult because of the inefficient processing and secretion of C96Y mutant proinsulin 2 (3) and the higher protein synthesis rate in Akita islets (Fig. 3*B*). To minimize this difference, the islets were incubated with brefeldin A, which induces disassembly of the Golgi apparatus and thereby inhibits protein secretion (21). These experiments confirmed that there were no distinct differences in the formation of intermolecular bonds between wild-type and C96Y proinsulin (data not shown). Thus, a thiol-mediated mechanism is unlikely to account for the retention and degradation of coexisting wild-type proinsulin in Akita β-cells.

To substantiate this notion, we constructed a mouse insulin 2 cDNA whose protein product harbors both C96Y (A7) and C31A (B7) mutations and expressed it in CHO cells. We reasoned that if the double mutations that eliminate free cysteine residues improve the secretion efficiency, then the formation of mispaired intra- or intermolecular disulfide bonds is responsible for the secretion block of the single C96Y mutant proinsulin 2. As we reported previously (3), C96Y proinsulin 2 was barely secreted into the media, in contrast to the wild type (Fig. 5). The double mutant proinsulin 2 was even less efficiently secreted than the single mutant, suggesting that the generation of unpaired cysteine is not responsible for the block in secretion of the single cysteine mutant.

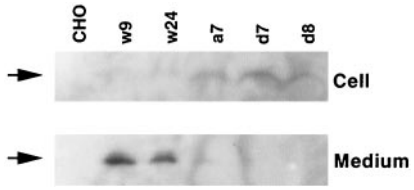

FIG. 5. Proinsulin 2 secretion from CHO cell lines. Parental CHO cells or those expressing wild-type (clones w9 and w24), C96Y (A7) single mutant (clone a7), or C96Y (A7) and C31A (B7) double mutant proinsulin 2 (clones d7 and d8) were incubated with serum-free media for 24 h. The cells (*upper panel*) were then solubilized, and the media (*lower panel*) were concentrated by 10% trichloroacetic acid. These samples were resolved with tricine-SDS-PAGE (16.5% polyacrylamide gel). Immunoblotting analysis was performed using anti–C-peptide antibodies. Arrows indicate the position of human proinsulin standard. Note that the wild-type proinsulin 2 is secreted more efficiently than the mutant proinsulin 2, despite the lower expression levels in the cells (see Fig. 1).

Effect of mutant proinsulin on the trafficking of SEAP. Given that proinsulin is a predominant protein product in β-cells, accumulation of nondegraded, misfolded proinsulin may clog the secretory pathway and lead to a reduction in the traffic of other critical secretory molecules. To explore this possibility, we expressed SEAP in isolated islets by recombinant adenovirus and measured its transport efficiency. The islets were incubated for 30 min under the basal condition and then for another 30 min in the presence of high K^+, and the immunoreactive insulin and SEAP enzyme activity were quantified. As expected, Akita islets showed significantly reduced insulin secretion in both the basal and high K^+–stimulated state compared with control islets (Fig. 6*A*). The fold stimulation elicited by high K^+, however, was not significantly different between these two islets (approximately fivefold). It should be noted that our anti-insulin antibodies do not react with the mutant form (3). Thus these findings indicated that coexisting wild-type insulin in Akita islets was normally secreted in a regulated fashion once it reached the secretory granules, although the absolute amount of insulin secreted was decreased. SEAP was secreted at a much higher level under the basal condition and was increased only 1.3-fold upon stimulation in control islets (Fig. 6*B*), indicating that it is secreted largely in a constitutive manner, as previously reported (15). The secretion efficiency of SEAP in Akita islets was significantly decreased (58–60% of control islets) under both the basal and stimulated conditions. This value of inhibition is an underestimate, however, as Akita islets contain relatively fewer β-cells (3) and are inevitably less pure because of deformation and denaturation (~30% of acinar, fat, and vascular cells are contaminated). Thus a relatively higher contribution from healthy non–β-cells in Akita islet preparations should augment the apparent SEAP transport efficiency. The reduction of SEAP transport suggests general and nonspecific dysfunction of organelles in secretory pathways.

Morphological changes in the β-cells. Because the secretion efficiency of SEAP is measured as the ratio of the amount in media to cells, its decrease in Akita islets cannot be explained by the reduction of islet cell mass, but instead should reflect the dysfunction of the individual cell. To substantiate this hypothesis, we next examined the morphology of β-cells from mice of different ages by

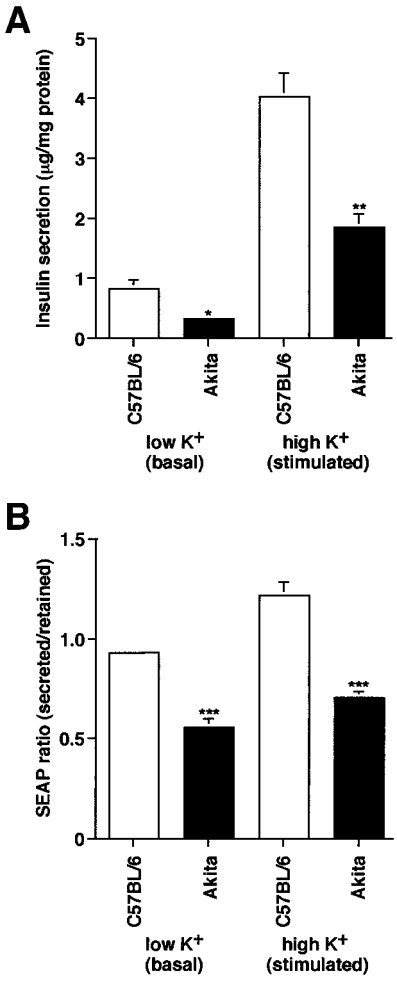

FIG. 6. Secretion of insulin and SEAP from pancreatic islets. Islets isolated from 12- to 14-week-old male control C57BL/6 (□) and Akita mice (■) were infected with recombinant adenovirus bearing SEAP cDNA. They were then incubated under a basal condition for 30 min followed by a second 30-min incubation in the presence of high K^+ (60 mmol/l). Immunoreactive insulin in the media was measured with anti-insulin antibodies and corrected by the protein content in the islet extracts (*A*). Note that the antibodies used did not recognize the C96Y mutant form (3). The SEAP enzymatic activity (optical density 405 per min) was measured, and the secretion was shown as a ratio of the activity secreted in media to that retained in cells in order to adjust for potential differences in the infection efficiency (*B*). The results are given as the mean ± SE of four independent experiments. *$P < 0.05$, **$P < 0.005$, ***$P < 0.0001$ versus control C57BL/6 islets in the same experimental condition, shown in the adjacent left column.

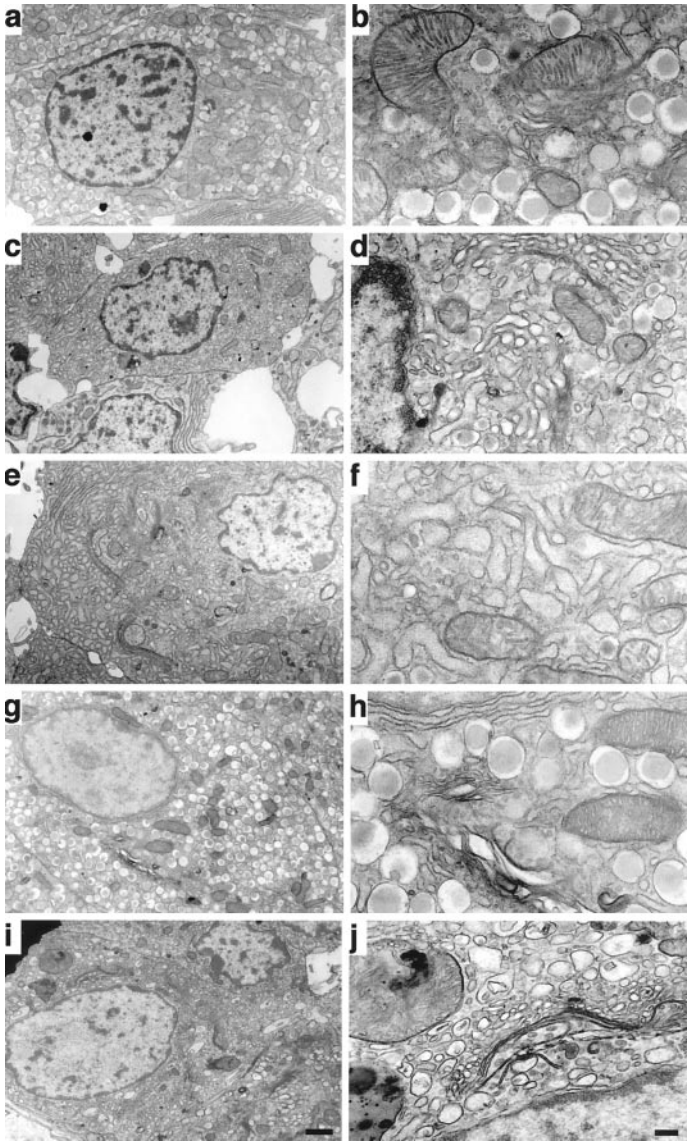

FIG. 7. Ultrastructural morphology of β-cells. Electron micrographs of the β-cells are taken from 4- (*a–d*), 13- (*e*,*f*), or 18-week-old (*g–j*) male C57BL/6 (*a*, *b*, *g*, and *h*) and Akita mice (*c–f*, *i*, and *j*). Parts *b*, *d*, *f*, *h*, and *j* (bar, 200 nm) represent higher magnification of *a*, *c*, *e*, *g*, and *i* (bar, 1 μm), respectively. Note that β-cells from 4-week-old Akita mice already show highly distended tubulovesicular structures and less granules and mitochondria (*c* and *d*). These features are universally seen in Akita β-cells. For example, in *c*, distended ER-like structures are seen in both the center and the adjacent left β-cells, although they are not seen in the adjacent right and bottom non–β-cells. In the older mice, the mitochondria are markedly swollen and denatured without distinct cristae (*i* and *j*). The nuclei of β-cells did not show condensed or fragmented chromatin.

electron microscopy. Control β-cells from mice at age 4 weeks were already equipped with numerous granules and mitochondria (Fig. 7*a* and *b*). At this age, when glucose levels begin to increase in Akita mice, β-cells had a much denser appearance, reflecting a reduced area of granule halos and enrichment of distended ER-like structures (Fig. 7*c* and *d*). In contrast, these morphological changes were not seen in adjacent non–β-cells (Fig. 7*c*). The lumina of ER-like organelles were progressively enlarged with age (Fig. 7*e* and *f*). Control β-cells from mice at age 18 weeks still bore abundant granules and mitochondria (Fig. 7*g* and *h*), whereas the cytoplasm of Akita β-cells was filled with vacuole-like structures, which comprise distended ER-like organelles and granules with remnant dense cores (Fig. 7*i* and *j*). Notably, the mitochondria were often swollen and denatured without distinct cristae, and enlarged lysosomes were often visible. The devastating changes in the organelle architecture were universally seen in Akita β-cells (see adjacent β-cells in Fig. 7*c*, *e*, and *i*). These morphological findings support the general and nonspecific impairment of secretory pathways of Akita β-cells, which is consistent with reduced SEAP transport.

Apoptosis of β-cells. High levels of ER stress can initiate cell death−inducing signals in higher eukaryotic cells (4,22). We examined TUNEL-positive β-cells in Akita and control mice (Fig. 8). There was a slight increase in TUNEL-positive β-cells in Akita mice at age 13 weeks: 20 apoptotic β-cells in 43 Akita islets (0.47 per islet) versus 7

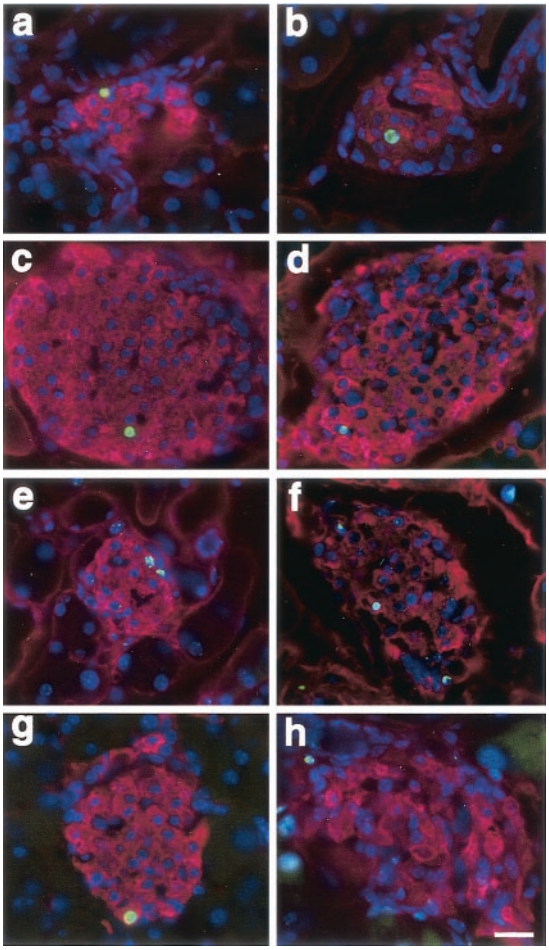

FIG. 8. Apoptosis in the pancreatic islets. Apoptosis in islets was detected by TUNEL labeling in C57BL/6 (*a*, *c*, and *g*) and Akita mice (*b*, *d–f*, and *h*) at age 4 (*a* and *b*), 13 (*c–f*), or 18 weeks (*g* and *h*). TUNEL-positive cells are detected by the fluorescein isothiocyanate tag (green). Whether such cells were β-cells or non–β-cells was confirmed by using immunostaining with anti-insulin and Red-X–labeled anti-guinea pig IgG antibodies (red). The nuclei of all cells were visualized with DNA-binding dye H33342 (Calbiochem-Novabiochem; blue). Examples of the islets containing apoptotic β-cells are shown, although most islets in sections do not contain TUNEL-positive cells. Bar, 20 μm.

apoptotic β-cells in 52 control islets (0.15 per islet). The number of apoptotic cells is expressed per whole islet examined three-dimensionally in each 4-μm serial section. Thus, the frequency of apoptotic events was fairly low, even in Akita β-cells. Although we also examined the pancreata from mice at ages 4 and 18 weeks, most islets again contained no or only a single TUNEL-positive cell, irrespective of age (data not shown, but see Fig. 8). Hoechst dye staining of nuclear chromatin consistently showed barely detectable levels of condensed or fragmented nuclear chromatin, which is a morphological characteristic of apoptotic cells, in either control or Akita β-cells (Fig. 8). Furthermore, electron microscopic analysis identified no nuclei having an apoptotic appearance (Fig. 7).

DISCUSSION

The mechanism by which the mutant manifests its pathology and affects the function of coexpressed wild-type protein remains uncharacterized, not only for diabetes in Akita mice but also for other dominant conformational diseases in humans. Several dominant-negative mechanisms have been postulated, such as a block in the synthesis of wild-type protein, aberrant interactions between mutant and wild-type precursors (the formation of inactive heterodimers), and cytotoxicity by mutant protein leading to the death of expressing cells.

Although there were theoretical grounds for expecting a decrease in protein synthesis in cells expressing the mutant proinsulin, this was not substantiated by the present results. Furthermore, again contrary to theoretical expectations, there was no major increase in cross-linked homo- or hetero-oligomers of the mutant proinsulin. Instead, we found that a fraction of wild-type proinsulin was degraded by the proteasome and, more surprisingly, that intermolecular disulfide bonds were formed during its normal folding process. These findings suggest that a portion of nascent wild-type proinsulin is misfolded, and that β-cells are continuously in a situation close to ER "overload." Several point mutations that result in amino acid substitutions within the proinsulin molecules are known in humans, although those involving disulfide bonds have not been reported (23). Minor conformational changes of these human mutant proinsulins may induce β-cell dysfunction in the long term. If a portion of misfolded protein is not successfully degraded and is gradually accumulated, it accounts for the delayed onset and autosomal dominant mode of inheritance of the disease.

It is possible that the intermolecular disulfide bonds observed in the two-dimensional SDS-PAGE analyses may represent links transiently formed during the physiological folding process between nascent proinsulin and molecular chaperones, such as protein disulfide isomerase, as previously shown for viral glycoproteins (24). The lack of discernible differences in the formation of these bonds between wild-type and C96Y proinsulin supports this idea, and also suggests that the cysteine at B7 in the mutant is left unpaired and is not actively involved in the formation of a tangle of disulfide isomers. However, considering the recent structural analyses of insulin analogs lacking the A7−B7 disulfide bond (7,8), the mutant proinsulin is likely to exhibit significantly enhanced exposure of nonpolar side chains, leading to aberrant self-association, even in the absence of disulfide bridges. This might account for the increased electron-dense deposits in the β-cells of Akita mice.

ER stress can initiate cell death pathways (4,22). Indeed, it has been shown recently that apoptosis is increased in β-cells of Akita mice at age 4 weeks and that overexpression of *Ins2*^{C96Y} induces apoptosis in the β-cell line MIN6 (9). We also detected a slight increase in apoptosis in Akita β-cells, but with a much lower frequency (< 1 cell per islet) than that reported previously (10–11 cells per islet) (9). Furthermore, electron microscopic analysis revealed no nuclear chromatin condensation or fragmentation, but instead necrotic-like features, such as mitochondrial swelling and dilation of ER-like organelles (25). These findings cannot, however, be taken to indicate that apoptosis is not a major cause of increased β-cell death in the Akita mouse, because it has been established by others (26) that apoptotic cells are cleared rapidly by macrophages in vivo.

Massive intracellular accumulation of misfolded proinsulin may affect the function of organelles in secretory pathways and interfere with the transport of other critical biosynthetic cargo (including integral membrane proteins). In fact, we found a partial but significant reduction in SEAP transport in Akita islets. The impairment of SEAP transport, which occurs through a constitutive secretory pathway, is consistent with the notion that misfolded proinsulin is accumulated in the early secretory pathway, before the trans-Golgi network, where SEAP is differentially sorted out from proinsulin. Even a partial blockade of SEAP transport implies general, wide-ranging dysfunction of secretory organelles, given that SEAP is considered properly folded and completely unrelated to insulin. It has recently been shown in yeast that some misfolded secretory proteins are not statically retained in the ER, but are dynamically packaged into COPII vesicles, transported to the Golgi apparatus, and retrieved via the retrograde transport pathway (27). Furthermore, degradation of these misfolded secretory proteins is shown to require transport between the ER and Golgi components (27,28). Therefore, the reduction in dynamic transport between the ER and Golgi, as suggested by our SEAP secretion assay, may further augment the accumulation of misfolded proteins. Alternatively, the number of vesicles budding from the ER may be reduced by expression of mutant proteins, as was previously shown in the case of a temperature-sensitive mutant of vesicular stomatitis glycoprotein and the PiZ variant of human α1-antitrypsin (29). The functional impairment of secretory pathways correlates with the morphological changes of Akita β-cells. Our electron microscopic analysis revealed a progressive deterioration of organelle architecture: distension of ER-like structure, a decrease in secretory granules, and swelling and denaturation of the mitochondria. It should be noted that these morphological changes were already detected in mice at age 4 weeks, when glucose intolerance develops in Akita mice. Our findings are consistent with the proposition that incorrectly folded proteins could interfere with the transport of other biosynthetic cargo molecules and thus exert a dominant effect on them.

In summary, the overall reduction of SEAP transport and the universal devastation in Akita mouse β-cell organelle architecture strongly suggest that these functional and morphological changes precede final sporadic cell death. Thus we propose that progressive organelle dysfunction of individual β-cells is primarily responsible for the disease phenotype of Akita mice. Further detailed analysis of the organelle function at each transport step in Akita β-cells should provide a valuable basis for the pathogenesis of other dominantly inherited conformational diseases in humans.

ACKNOWLEDGMENTS

This work was supported by a grant-in-aid for scientific research from the Ministry of Education, Culture, Sports, Science, and Technology of Japan. It was also supported in part by grants from the Japan Diabetes Foundation, Suzuken Memorial Foundation, Yamanouchi Foundation for Research on Metabolic Disorders, and Japan Insulin Study Group Award, to T.I., and from the Swiss National Science Fund (3200-061776.00) to P.A.H.

We thank Z. Yi (Institute for Molecular and Cellular Regulation, Gunma University) for amplifying adenovirus. We also thank Dr. A. Koizumi (Kyoto University School of Medicine), Dr. H. Gomi, A. Tsunoda, and M. Hosoi (Institute for Molecular and Cellular Regulation, Gunma University) for their generous support.

REFERENCES

1. Aridor M, Balch WE: Integration of endoplasmic reticulum signaling in health and disease. *Nat Med* 5:745–751, 1999
2. Yoshioka M, Kayo T, Ikeda T, Koizumi A: A novel locus, *Mody4*, distal to D7Mit189 on chromosome 7 determines early-onset NIDDM in nonobese C57BL/6 (Akita) mutant mice. *Diabetes* 46:887–894, 1997
3. Wang J, Takeuchi T, Tanaka S, Kubo S-K, Kayo T, Lu D, Takata K, Koizumi A, Izumi T: A mutation in the insulin 2 gene induces diabetes with severe pancreatic β-cell dysfunction in the *Mody* mouse. *J Clin Invest* 103:27–37, 1999
4. Kaufman RJ: Stress signaling from the luman of the endoplasmic reticulum: coordination of gene transcriptional and translational controls. *Genes Dev* 13:1211–1233, 1999
5. Mori K: Tripartite management of unfolded proteins in the endoplasmic reticulum. *Cell* 101:451–454, 2000
6. Ellgaard L, Molinari M, Helenius A: Setting the standards: quality control in the secretory pathway. *Science* 286:1882–1888, 1999
7. Guo Z-Y, Feng Y-M: Effects of cysteine to serine substitutions in the two inter-chain disulfide bonds of insulin. *Biol Chem* 382:443–448, 2001
8. Hua Q-X, Nakagawa SH, Jia W, Hu S-Q, Chu YC, Katsoyannis PG, Weiss MA: Hierarchical protein folding: asymmetric unfolding of an insulin analogue lacking the A7–B7 interchain disulfide bridge. *Biochemistry* 40:12299–12311, 2001
9. Oyadomari S, Koizumi A, Takeda K, Gotoh T, Akira S, Araki E, Mori M: Targeted disruption of the *Chop* gene delays endoplasmic reticulum stress-mediated diabetes. *J Clin Invest* 109:525–532, 2002
10. Zinszner H, Kuroda M, Wang X, Batchvarova N, Lightfoot RT, Remotti H, Stevens JL, Ron D: CHOP is implicated in programmed cell death in response to impaired function of the endoplasmic reticulum. *Genes Dev* 12:982–995, 1998
11. McCullough KD, Martindale JL, Klotz L-O, Aw T-Y, Holbrook NJ: Gadd153 sensitizes cells to endoplasmic reticulum stress by down-regulating Bcl2 and perturbing the cellular redox state. *Mol Cell Biol* 21:1249–1259, 2001
12. Leroux L, Desbois P, Lamotte L, Duvillié B, Cordonnier N, Jackerott M, Jami J, Bucchini D, Joshi RL: Compensatory responses in mice carrying a null mutation for *Ins1* or *Ins2*. *Diabetes* 50:S150–S153, 2001
13. Yi Z, Yokota H, Torii S, Aoki T, Hosaka M, Zhao S, Takata K, Takeuchi T, Izumi T: The Rab27a/granuphilin complex regulates the exocytosis of insulin-containing dense-core granules. *Mol Cell Biol* 22:1858–1867, 2002
14. Chen W, Helenius J, Braakman I, Helenius A: Cotranslational folding and calnexin binding during glycoprotein synthesis. *Proc Natl Acad Sci U S A* 92:6229–6233, 1995
15. Molinete M, Lilla V, Jain R, Joyce PBM, Gorr S-U, Ravazzola M, Halban PA: Trafficking of non-regulated secretory proteins in insulin secreting (INS-1) cells. *Diabetologia* 43:1157–1164, 2000
16. Cullen BR, Malim MH: Secreted placental alkaline phosphatases as a eukaryotic reporter gene. *Methods Enzymol* 216:362–368, 1992
17. Plemper RK, Wolf DH: Retrograde protein translocation: ERADication of secretory proteins in health and disease. *Trends Biochem Sci* 24:266–270, 1999
18. Lee DH, Goldberg AL: Proteasome inhibitors: valuable new tools for cell biologists. *Trends Cell Biol* 8:397–403, 1998
19. Shi Y, Vattem KM, Sood R, An J, Liang J, Stramm L, Wek RC: Identification and characterization of pancreatic eukaryotic initiation factor 2α-subunit kinase, PEK, involved in translational control. *Mol Cell Biol* 18:7499–7509, 1998
20. Harding HP, Zhang Y, Ron D: Protein translation and folding are coupled by an endoplasmic-reticulum-resident kinase. *Nature* 397:271–274, 1999
21. Jackson CL, Casanova JE: Turning on ARF: the Sec7 family of guanine-nucleotide-exchange factors. *Trends Cell Biol* 10:60–67, 2000
22. Ferri KF, Kroemer G: Organelle-specific initiation of cell death pathways. *Nat Cell Biol* 3:E255–E263, 2001
23. Steiner DF, Tager HS, Chan SJ, Nanjo K, Sanke T, Rubenstein AH: Lessons learned from molecular biology of insulin-gene mutations. *Diabetes Care* 13:600–609, 1990

24. Molinari M, Helenius A: Glycoproteins from mixed disulphides with oxidoreductases during folding in living cells. *Nature* 402:90–93, 1999
25. Clarke PG: Developmental cell death: morphological diversity and multiple mechanisms. *Anat Embryol* 181:195–213, 1990
26. O'Brien BA, Huang Y, Geng X, Dutz JP, Finegood DT: Phagocytosis of apoptotic cells by macrophages from NOD mice is reduced. *Diabetes* 51:2481–2488, 2002
27. Vashist S, Kim W, Belden WJ, Spear ED, Barlowe C, Ng DTW: Distinct retrieval and retention mechanisms are required for the quality control of endoplasmic reticulum protein folding. *J Cell Biol* 155:355–367, 2001
28. Caldwell SR, Hill KJ, Cooper AA: Degradation of endoplasmic reticulum (ER) quality control substrates requires transport between the ER and Golgi. *J Biol Chem* 276:23296–23303, 2001
29. Aridor M, Bannykh SI, Rowe T, Balch WE: Cargo can modulate COPII vesicle formation from the endoplasmic reticulum. *J Biol Chem* 274:4389–4399, 1999